NONLINEAR SIMULATION OF RC STRUCTURES USING APPLIED ELEMENT METHOD

Hatem TAGEL-DIN[1] and Kimiro MEGURO[2]

[1] Member of JSCE, Ph.D., Post-Doctorate Fellowship, Institute of Industrial Science,
The University of Tokyo (4-6-1 Komaba, Meguro-ku, Tokyo 153-8505, Japan)
[2] Member of JSCE, Dr. of Eng., Associate Professor, International Center for Disaster-Mitigation Engineering
Institute of Industrial Science, The University of Tokyo (4-6-1 Komaba, Meguro-ku, Tokyo 153-8505, Japan)

A new extension for the Applied Element Method (AEM) is introduced. Using this method, the structure is modeled as an assembly of distinct elements made by dividing the structural elements virtually. These elements are connected by distributed springs in both normal and tangential directions. This paper describes the applicability of the AEM for different fields of analysis and structure types and it deals with the formulations used for RC structures under monotonic loading. It is proved in this paper that the structural failure behavior including crack initiation and propagation can be simulated accurately with reasonable CPU time and without any use of complicated material models.

Key Words: *Applied Element Method, AEM, nonlinear analysis, fracture analysis, reinforced concrete*

1. INTRODUCTION

The formulation of the Applied Element Method (AEM) for elastic materials was introduced in Refs. 1) and 2). It was proved that displacements, internal stresses and strains could be calculated accurately assuming elastic material behavior. In addition, the effects of Poisson's ratio could be considered. This paper gives good indication that accurate results can be also obtained in nonlinear cases.

Many numerical techniques exist for nonlinear analysis of structures. The most famous one is the Finite Element Method (FEM). FEM for nonlinear case has been developed and used widely. Analysis of continuum media, like steel structures, using the FEM showed very high accuracy. Analysis of cracked media, like reinforced concrete, is very complicated because the FEM assumes that the structure medium is continuum or uncracked. This means that special techniques should be used to consider the effects of cracks. Mainly two groups of techniques that consider the effect exist. The first group deals with mechanical behavior of cracks by methods called "Smeared cracks[3]". These methods consider cracks by adopting its effect on the stiffness and stress-strain relations. These techniques showed high accuracy in calculating

displacements and failure loads. However, they have four main disadvantages:
1. Models used are relatively complicated.
2. Fracture behavior cannot be accurately followed in "smeared" crack zones.
3. Special elements should be used in the location of dominant cracks, like interface cracks between structural elements. Neglecting the effects of interface cracks affects greatly the results[2]. Modeling requires previous knowledge about the location and direction of propagation of cracks.
4. Reinforcement data are input as average values within a certain area. This means that stresses and strains obtained by these methods are also average values. Following stresses and strains of a specific steel bar and/or concrete leads to many complications in modeling before the analysis and also leads to increase the CPU time required for the analysis.

The other group is mainly for discrete crack modeling[4,5]. With these methods, each crack is taken into account as a discrete crack whose location and propagation direction, in most of FEM codes, should be defined before the analysis. They are suitable only in case of few numbers of cracks. Carrying out complicated failure behavior of reinforced concrete elements using FEM is very difficult. Because of limitations in representation of
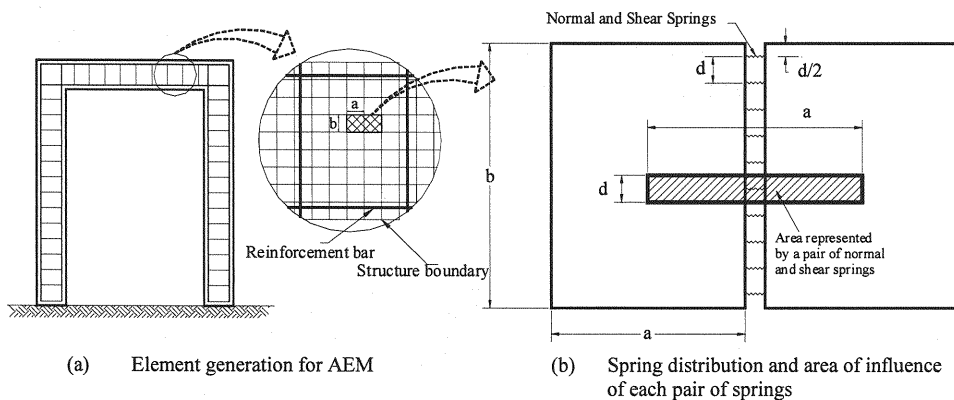
(a)   Element generation for AEM

(b)   Spring distribution and area of influence of each pair of springs

Fig. 1   Modeling of structure to AEM

fracture behavior of the RC structures, analyses using the FEM were mainly performed in small deformation range and till the beginning of collapse of the structure.

To deal with these problems, many other methods were developed. The Rigid Body and Spring Model, RBSM[6], is one of them. The main advantage of this method is that it simulates the cracking process with relatively simple technique compared to the FEM, while the main disadvantages is that crack propagation depends mainly on the shape, size and arrangement of the elements used[7), 8)]. One of the recent methods to deal with fracture analysis of concrete is the Modified or Extended Distinct Element Method, MDEM[9] or EDEM[10]. This method can follow the highly non-linear geometric changes of the structure during failure, however, the main disadvantages of this method are that, in some cases, accuracy is not enough for quantitative discussion and it needs relatively long CPU time compared with the FEM and RBSM. In addition, the accuracy of the EDEM in small deformation range is less than that of the FEM.

This paper introduces the numerical technique to deal with nonlinear analysis of structures. To show the strong points of the proposed method, simulations are performed using RC structure models and results are compared with those obtained by other numerical techniques whenever it is possible. Using the proposed method, highly nonlinear behavior, i.e. crack initiation, crack propagation till the beginning of collapse process of the structure can be followed accurately with reasonable CPU time. Behavior of total collapse process of structure can also be followed by the method with some additional considerations and the formulations required for large deformation analysis. They are introduced by other publications.
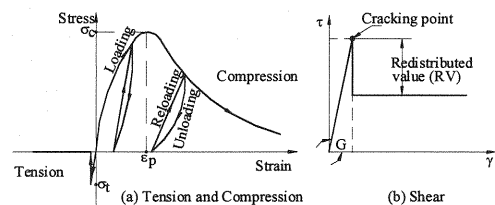

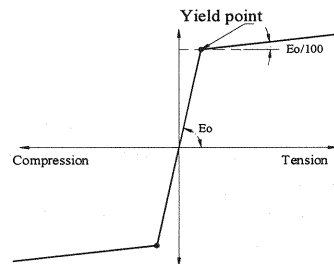**Fig. 2** Tension, compression and shear models for concrete

Fig. 3 Stress-strain relation for steel

2. ELEMENT FORMULATION & MATERIAL MODELING

In AEM, the structure is modeled as an assembly of small elements which are made by dividing the structure virtually, as shown in **Fig. 1 (a)**. Two elements shown in figure are assumed to be connected by pairs of normal and shear springs set at contact locations which are distributed around the element edges. Stresses and strains are defined based on the displacements of the spring end points which are located along the axis passing through centroid of the element. Three degrees of freedom are assumed for each element. In this formulation, we just use plain concrete model and steel model and the total behavior is the summation of both. Simply, if reinforcement exists, it affects the stiffness matrix of the element. Therefore, total

behavior of reinforced concrete with some reinforcement ratio can be simulated automatically. For other details like calculation of spring stiffness, please refer to Ref. 1).

As a material modeling of concrete under compression condition, Maekawa compression model[3], as shown in **Fig. 2 (a)**, is adopted. In this model, the initial Young's modulus, the fracture parameter, representing the extent of the internal damage to concrete, and the compressive plastic strain are introduced to define the envelope for compressive stresses and compressive strains. Therefore unloading and reloading can be conveniently described. For more details, refer to Ref. 3). The tangent modulus is calculated according to the strain at the spring location. To consider the confinement effects in compression zones, Kupfer[11] biaxial failure function is adopted. A modified compressive strength, f_{ceq}, is calculated using Eq. (1). This indicates that the compressive resistance associated with each spring is variable and depends mainly on the stress situation at the spring location. To determine the principal stress components σ_1 and σ_2, refer to Sec. 3.

$$f_{ceq} = \frac{1 + 3.65(\sigma_1/\sigma_2)}{(1 + \sigma_1/\sigma_2)^2} f_c \qquad (1)$$

After peak stresses, spring stiffness is assumed as 0.1% of the original value. This small value is assumed to avoid negative stiffness. This results in difference between calculated stress and stress corresponds to the spring strain. These residual stresses are redistributed by applying the force in the reverse direction. For concrete springs subjected to tension, spring stiffness is assumed as the initial stiffness till reaching the cracking point. After cracking, stiffness of springs subjected to tension is set to be zero. For reinforcement, bi-linear stress strain relation is assumed. After yield of reinforcement, steel spring stiffness is assumed as 1% of the initial stiffness as shown in **Fig. 3**. As the range of this paper is nonlinear behavior of structure in static condition, cut of reinforcement is not modeled in this present formulation. Because the behavior of the structure becomes mainly dynamic and the static stiffness matrix becomes singular in most of cases.

3. FAILURE CRITERIA

One of the main problems associated with the use of elements having three degrees of freedom is the modeling of diagonal cracking. Applying Mohr-Coulomb's failure criteria calculated from normal
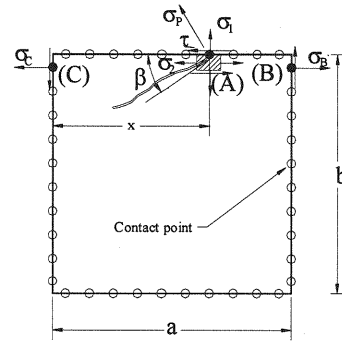

Fig. 4 Principal Stress determination

(a) Redistribution of springs forces at the crack faces

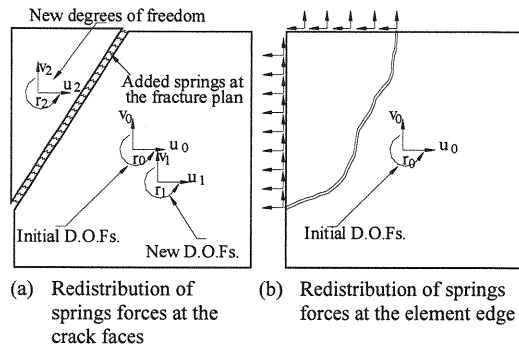(b) Redistribution of springs forces at the element edge

Fig. 5 Different strategies to deal with cracking

and shear springs, not based on principal stresses, has some problems. When the structure is really composed of individual elements, such as granular material or brick masonry buildings, Mohr-Coloumb's failure criteria is reasonable. However, when we use elements by dividing the structure virtually, which is not really composed of elements, for convenience of numerical simulation, adopting Mohr-Coloumb's failure criteria leads to inaccurate simulation of fracture behavior of the structure.

In the AEM, it was proved in Ref. 2) that stresses and strains around each element could be calculated accurately. The idea of the proposed technique is how to use the calculated stresses around each element to detect the occurrence of cracks. To determine the principal stresses at each spring location, the following technique is used. Referring to **Fig. 4**, the shear and normal stress components (τ and σ_1) at point (A) are determined from the normal and shear springs attached at the contact point location. The secondary stress (σ_2) can be calculated by Eq. (2) from normal stresses at the points (B) and (C), as shown in **Fig. 4**.

$$\sigma_2 = \frac{x}{a}\sigma_B + \frac{(a-x)}{a}\sigma_C \qquad (2)$$

The principal tension is calculated:

$$\sigma_p = \left(\frac{\sigma_1 + \sigma_2}{2}\right) + \sqrt{\left(\frac{\sigma_1 - \sigma_2}{2}\right)^2 + (\tau)^2} \qquad (3)$$

The value of principal stress (σ_p) is compared with the tension resistance of the studied material. When σ_p exceeds the critical value of tension resistance, the normal and shear spring forces are redistributed in the next increment by applying the normal and shear spring forces in the reverse direction. These redistributed forces are transferred to the element center as a force and moment, and then these redistributed forces are applied to the structure in the next increment.

The redistribution of spring forces at the crack location is very important for following the proper crack propagation. For the normal spring, the whole force is redistributed to have zero tension stress at the crack faces. Although shear springs at the location of tension cracking might have some resistance after cracking due to the effect of friction and interlocking between the crack faces, the shear stiffness is assumed zero after crack occurrence. To consider the effects of friction and interlocking, a redistributed value (RV), shown in **Fig. 2 (b)**, is adopted. For springs subjected to compression, Mohr-Coulomb's failure criterion is used for compression shear failure. When the spring reaches the compression shear failure, the shear force is redistributed and shear stiffness is assumed zero in later increments. It should be emphasized that adopting the "RV" factor is an approximation and research is still needed to cover accurately the post-cracking shear behavior. The value of RV adopted in the analyses is 0.5.

Referring to **Fig. 4**, local crack inclination angle (β) to the element edge direction can be calculated as follows:

$$\tan(2\beta) = \left(\frac{2\tau}{\sigma_1 + \sigma_2}\right) \qquad (4)$$

Having zero shear stress means that the crack direction is coincident with the element edge direction. In shear dominant zones, the crack direction is dominant by shear stress value. To represent the occurrence of the cracks, two main techniques can be used. The first one is to break the element into two segments, as shown in **Fig. 5 (a)**, and each of them has three degrees of freedom. Redistribution of tension stresses is made at the principal tension stress plane and zero shear plane. Although this solution has four advantages which are listed below, it has many complications.
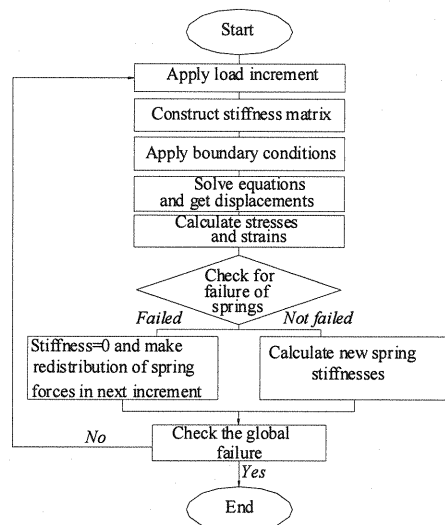1. The redistribution of tension stress is accurate.

Fig. 6 Flow of analysis

2. Crack direction inside the element can be represented accurately.
3. Crack width can be calculated accurately and hence, shear transfer and shear softening process can be simulated.
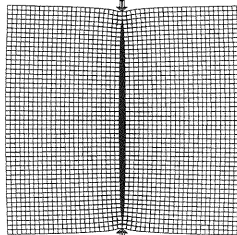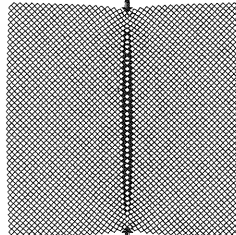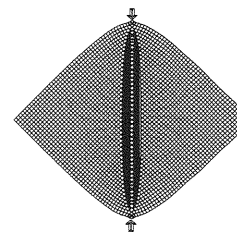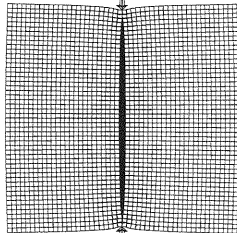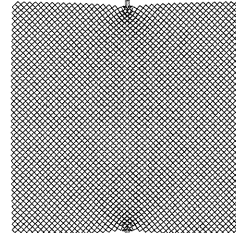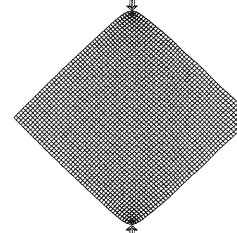4. Compression shear type of failure can be also simulated accurately.

Complications are:
1. The number of elements increases too much, especially if the elements used are small and the number of cracks becomes large.
2. Time of analysis increases after cracking because the number of elements increases.
3. The stiffness of springs at the cracked elements cannot be calculated accurately as before cracking. The reason is simply because each spring cannot simulate a certain area like before cracking[2].
4. In case of cyclic loading, successive cracking of the same elements leads to drastic decrease in the accuracy of solution.
5. Numerical errors arise if the elements after cracking have small aspect ratio.

The technique above requires some extensive research to overcome these problems. The alternative, refer to **Fig. 5 (b)**, does not have the previous complications. The idea is simple by assuming that failure inside the element is represented by failure of attached springs. This means that if a spring fulfills the failure criterion, the following steps are adopted:
1. Make redistribution of spring force.
2. Set failed springs stiffness equal to zero.

Table 1 Brazilian test results of specimens

Fracture Criterion	Case (1)	Case (2)	Case (3)
Number of elements	2500	3280	3280
AEM (Principal Stress)			
Failure Load	125 kN	125 kN	117 kN
RBSM or DEM type (Normal and Shear Stresses)			
Failure Load	125 kN	*Not failed*	*Not failed*

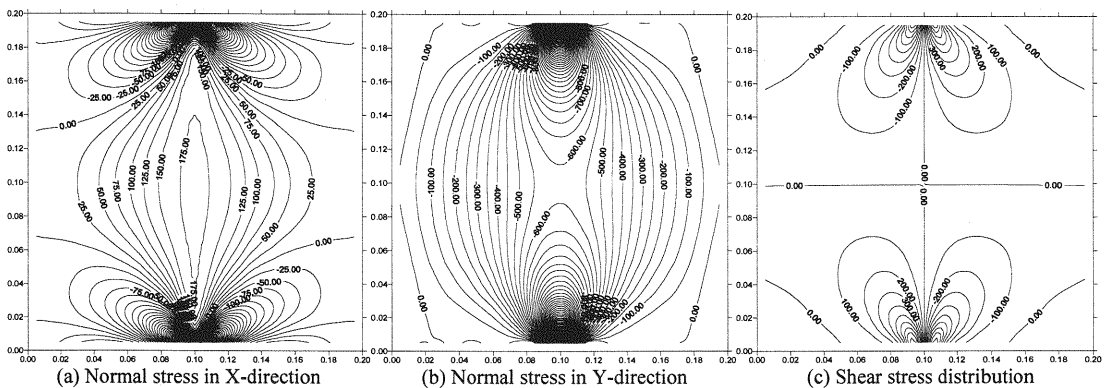(a) Normal stress in X-direction   (b) Normal stress in Y-direction   (c) Shear stress distribution

Fig. 7 Stress contours for a concrete cube subjected to concentrated loads (Dimensions are in meters and stresses, x 10kN/m^2)
(All contours are draw at load-level 120 kN in Case (1), before cracking occurrence)

This technique is simple and has the advantage that no special treatment is required to represent the cracking. In cases when the shear stresses are not dominant, like case of slender frames, the angle (β) tends to be zero. This indicates that the crack is parallel to the element edge and hence, high accuracy is expected. However, the main disadvantage of this technique is that the crack width cannot be calculated accurately. This indicates that post fracture behavior parameters that depends on the crack width, like shear transfer and shear softening, can not be simulated accurately. Compression shear failure also cannot be simulated accurately if the fracture plane is not parallel to element edges.
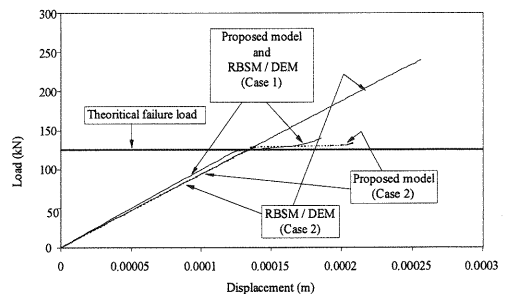
Fig. 8 Load-displacement relation for a concrete specimen using different techniques
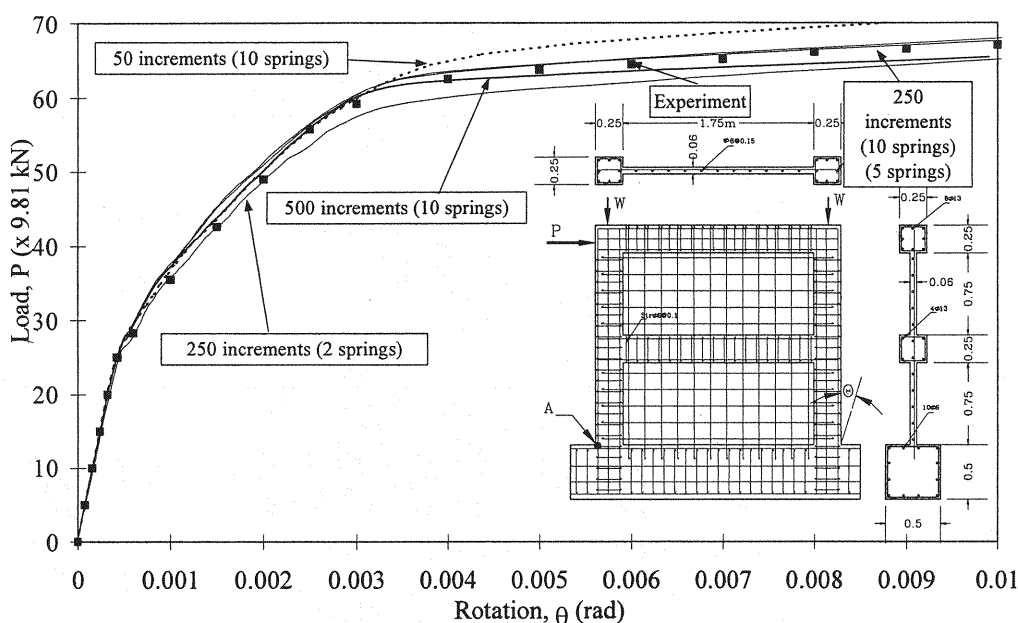
Fig. 9 Relation between load and wall rotation

4. FLOW OF THE METHOD

The flow chart of the numerical technique is shown in **Fig. 6**. This figure shows the modifications made to the program in elastic material case to consider nonlinear material effects. For more details about the flow of the analysis in elastic case, refer to Ref. 1). In each increment, stresses and strains are calculated for reinforcement and concrete springs. In case of springs subjected to tension, the failure criterion is checked, refer to Sec. 3). For springs subjected to compression, new tangent stiffness is calculated using the model illustrated in Sec. 2. For steel springs, tangent stiffness is determined from the bi-linear stress-strain relation, shown in **Fig. 3**. The spring stiffness matrices are constructed and assembled in the global matrix at each increment.

5. VERIFICATION WITH EXPERIMENTS AND OTHER NUMERICAL TECHNIQUES

The main objective of this section is to verify the accuracy of the proposed method in monotonic static loading condition. The results are compared also with other numerical techniques whenever possible. Those simulations using different types of 2-D models show the strong and weak points of the proposed technique.

(1) Effect of element arrangement

To verify the accuracy of the proposed method in comparison with other numerical techniques using rigid elements, such as RBSM and DEM, Brazilian test simulation is performed using square shaped concrete specimens subjected to concentrated loads. Three different mesh configurations are used. In Case (1), the elements are set parallel to the specimen edges, while in the second case, the elements are 45 degrees inclined to the specimen edges. In the third case, the load is applied to the diagonal of the square and the elements are parallel to the specimen edges. The distance between loading points is 20 cm in all cases and 10 springs were set between each two adjacent faces. The specimen thickness is assumed as 20 cm. Tension resistance is assumed as 2000 kN/cm². The results are summarized in **Table 1**. Theoretical failure load calculated by using the formula $P = \sigma_t \times \pi \times D \times L/2.0$ is 125 kN in Cases (1) and (2). Assumed material property is same in all the numerical models. In this simulation, compression failure under the applied load is not permitted. This effect can be seen after the failure load.

From the results, it can be noticed easily that the obtained failure load by the proposed model does not change for different element arrangement, while failure load can not be calculated by RBSM or DEM for 45° element discretization of Case (2). Although the normal and shear stress as applying to elements are different in Cases (1) and (2), the principal stresses, which dominate the occurrence of cracking,

do not change with the AEM. This means that results obtained by RBSM or DEM depend mainly on the element discretization[8]. This is mainly due to the use of Mohr-Coloumb's failure criterion based on two components of stresses (not based on principal stresses). This makes the results depend mainly on element shape and arrangement. Application of Mohr-Coloumb's failure criterion is suitable only for brick masonry type of structures but not suitable for continuum materials whose cracking behavior is dominant by the principal stresses.

Stress contours, σ_x, σ_y, τ_{xy} for Case (1) before cracking are shown in **Fig. 7**. It is obvious that stresses in x-direction in the middle of the specimen are tension while the stresses are mainly compression under the load. Stresses (σ_y) are the maximum under the applied load and stress contours diverge till reaching the middle of the specimen. Shear stresses are the maximum under the loading point and it has almost no effect away from the applied concentrated load.

(2) Two storied RC wall structure

The simulation results are compared with the experimental results of a two-storied RC wall structure. The size and shape of the wall, reinforcement and loading location are shown in **Fig. 9**. For more details about the experiment, refer to Ref. 12). The wall is modeled using 1,845 square shaped elements. The number of springs between each two adjacent faces is 10. The material properties used are decided by following Ref. 12) as follows: σ_y (for D6)=3,740 x 9.81 N/cm^2 while σ_y (for D13)=3,240 x 9.81 N/cm^2, σ_c=233 x 9.81 N/cm^2, σ_t=21.3 x 9.81 N/cm^2 and E_c=1940 kN/cm^2.

The wall is loaded by two permanent vertical weight (W) together with a horizontal load "P". Each vertical weight is equal to 187.5 kN. These loads are kept constant during the experiment.

Figure 9 shows a comparison between measured and calculated load-rotation relations. First, to discuss the effects of load increment in failure process, three models of different load increments, calculated by dividing the estimated failure (700 kN) load by 50, 250 and 500, with the constant number (10) of springs were used. Next, to study the effects of the number of connecting springs between faces, additional simulations were carried out using the case of 250 load increment with 5 and 2 springs between faces and the results are compared with those obtained with 10 springs. The failure loads calculated in all cases are within the range of 640 to 700 kN while the measured one was 670 kN. The calculated failure load using the FEM was 640 kN[2].
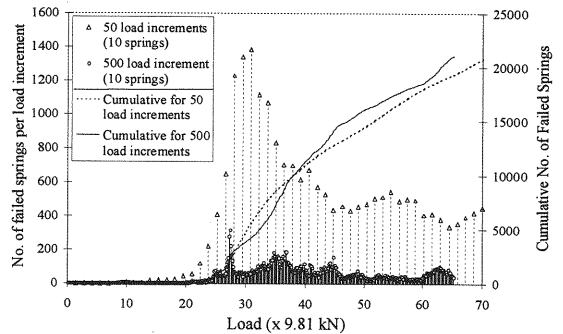

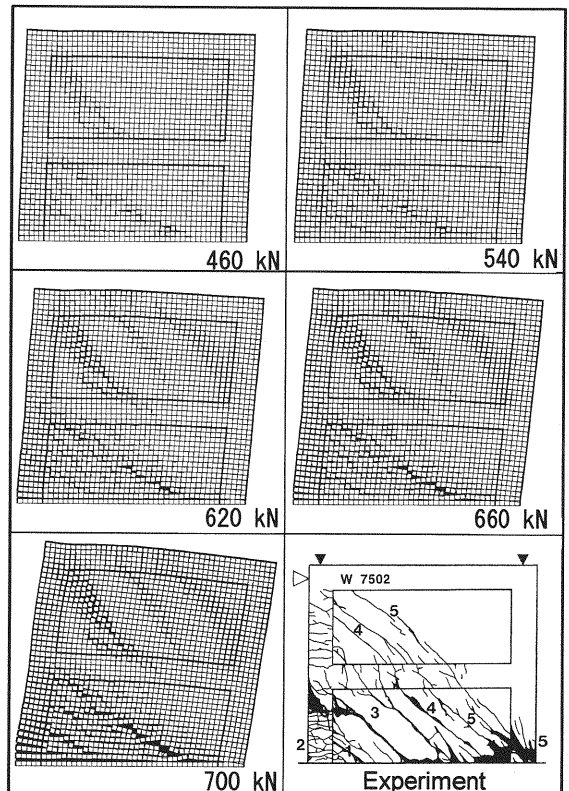**Fig. 10** Relation between load and the number of failed springs

Fig. 11 Deformed shape and crack locations of 2-storied RC wall structure (in case of 500 increments with 10 springs between each two adjacent faces, illustration scale factor=30)

In general, the calculated failure loads are very close to the measured one. The results of 50, 250 and 500 increments are almost congruent up to at least 95% of failure load. As the CPU time is proportional to the number of load increments, the CPU time in the case of 500 increments is about 10 times longer than that of 50 increments. To avoid long CPU time, relatively large value of load increment can be used till about 90% of expected failure load. From **Fig. 7**, the agreement between experimental and numerical
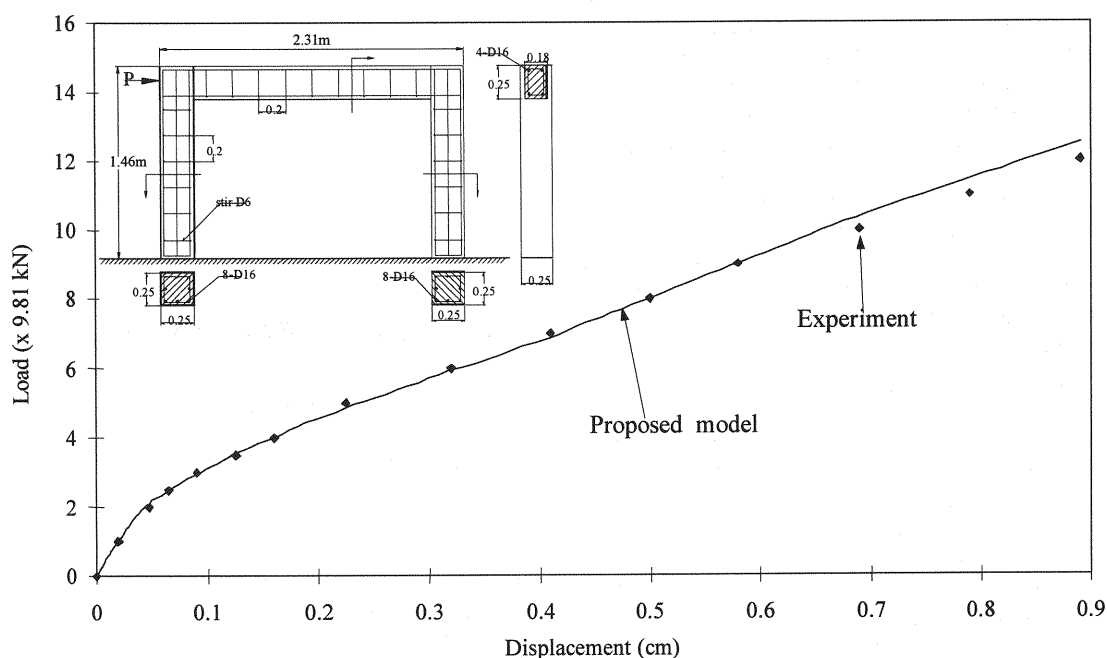
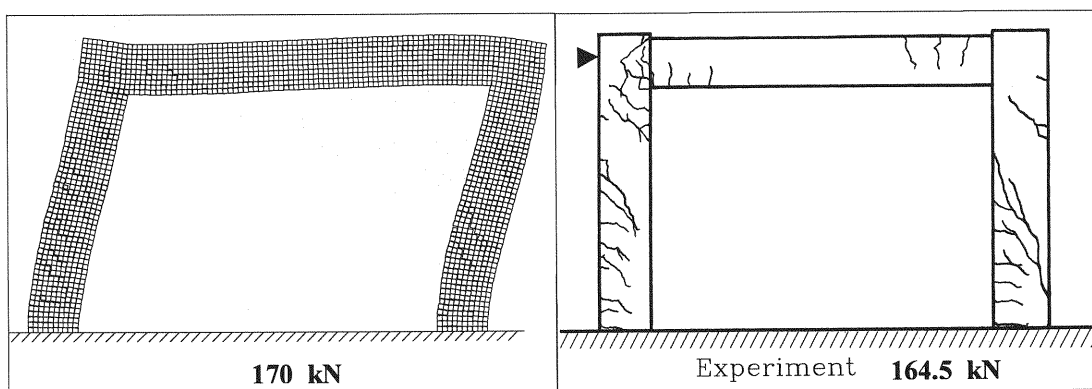**Fig. 12** Load-displacement relation of RC frame

Fig. 13 Deformed shape and crack patterns of RC frame (illustration scale factor =50)

results is fairly good for 250 increments with 10 or 5 connecting springs.

Surprisingly, for the case of 250 increments with only 2 springs connecting each two adjacent faces, the results are also reliable till reaching failure of the structure. It is also noted that using large sized load increments results in slightly higher failure load (700 kN) while using a few number of connecting springs gives slightly lower one (640 kN). Although the number of connecting springs affects directly the calculated rotational stiffness[1], it does not affect the result as the element size used in the analysis is small compared to the structure size. This means that the proposed model gives reliable results even when using a few number of connecting springs or relatively large sized load increments. Although increasing the number of springs leads to increasing the calculation time required for assembling the global stiffness matrix, the time required for solving equations, which is dominant when the number of elements is large, does not change because the number of degrees of freedom is independent of the number of springs used. This means that larger number of springs between edges can be used without significant change of the CPU time. On the other hand, when the total number of connecting springs used is large, computer memory capacity required becomes large.
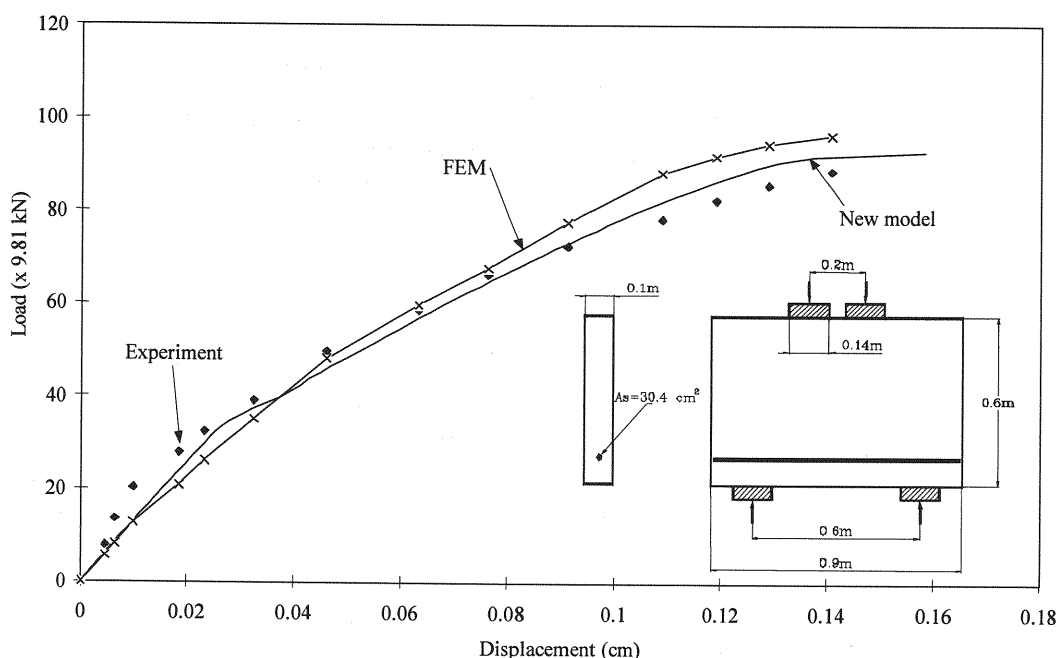
Fig. 14 Relation between load and displacement under the constant rate loading for RC deep beam

Figure 10 shows the relation between load and the number of failed springs for each increment. Cumulative curves also show the total number of failed springs till that increment. Excessive cracking begins to appear when the applied load is about 280 kN. At the same load, behavior of the structure begins to be highly nonlinear. In case of large value of load increment, many springs reach the failure criteria at the same increment and hence, the size of the new fracture zone developed each increment becomes larger. This indicates that the crack is not localized at a certain line, but in a narrow zone. Increasing the value of the applied load increment leads to increase the width of the zone representing the crack. This illustrates why the total number of failed springs in case of 50 increments (load increment is large) is greater than that of 500 load increments when fracture process starts.

Figure 11 shows the deformed shape during the application of load in case of 500 load increments with 10 springs. The location of cracks and crack propagation can be easily observed and they are very similar to those obtained from the experiment. The cracks are divided into three groups. The first group is the diagonal tension cracks, which appears mainly in the thin wall elements. It is obvious that diagonal tension cracks in the lower wall elements are wider than those in the upper wall. The second
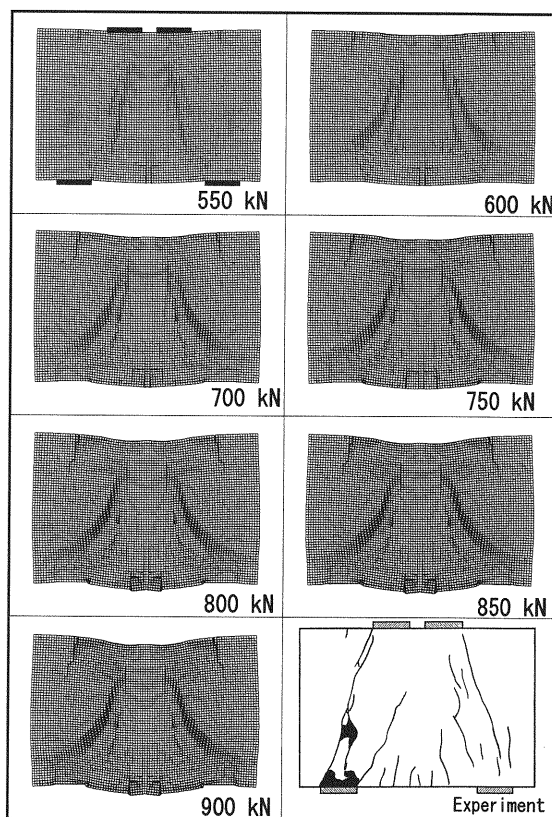

Fig.15 Deformed shape and crack pattern of deep beam
(illustration scale factor=40)

group of cracks is bending cracks in the columns and at the beam-column connections. Before failure, yield of column reinforcement occurs and hence, the crack width in the lower portion of the left column becomes wider. The third group is the crushing of concrete at the lower elements of the right column. Crushing of concrete can be noticed easily at the locations of overlapping between elements.

The above mentioned discussions show that the proposed model can be applied for fracture behavior of RC structures, such as, failure load, deformations, crack generation, crack location and propagation, etc. It should be emphasized that although the shape of elements used in the simulations is square, it does not affect the crack generation or crack propagation in the material. Diagonal cracks, as shown in **Fig. 11**, coincide well with those obtained from the experiment. In the simulation using rigid elements, like RBSM[6], shapes and distributions of elements should be decided before the simulation based on the assumption that crack locations and direction of propagation are known.

(3) RC frame subjected to lateral loads

The dimensions, loading conditions and reinforcement details[13] are shown in **Fig. 12**. The material properties used in the simulation are decided by Ref. 13) as follows: σ_y=4,620 x 9.81 N/cm^2, σ_c=186 x 9.81 N/cm^2, σ_t=15 x 9.81 N/cm^2 (σ_t is assumed to fit the crack initiation in the experiment) and E_c=2540 kN/cm^2

The frame is modeled using 1,880 elements with 10 connecting springs. The load is applied at the shown location in 200 increments. All reinforcement details, including stirrups location and diameters, are taken into account. **Figure 12** shows the relation between load and deformation calculated by the proposed model and measured by the experiment. An excellent agreement between the two results has been achieved. **Figure 13** shows the deformed shape and crack location at the final stage of simulation and experiment. Good agreement between the measured and calculated crack locations, crack inclination and crack length can also be obtained. In both experiment and numerical simulation, failure occurs near the base and at connections. The left connection is subjected to opening moments while the right one subjected to closing moments. In both cases, cracking obtained from the model agrees well with that obtained from the experiment. Also, the cracks of the left column, subjected to tension, are wider than those of the right one.

(4) RC deep beam

The next verification example is an RC deep beam[14]. Dimensions, loading conditions and reinforcement details are shown in **Fig. 14**. The material properties of the beam are the same as those in Ref 14) as follows: σ_y =3,890 x 9.81 N/cm^2, σ_c =666 x 9.81 N/cm^2, σ_t =30 x 9.81 N/cm^2 and E_c=3000 kN/cm^2 (σ_t and E_c are assumed to fit the crack initiation and initial stiffness, repectively, in the experiment).

Numerical analysis is performed for half of the beam only because of symmetry. The model is divided into 2,700 square elements. The number of springs between each two adjacent element faces is 10. Analysis of such type of problems is relatively difficult because reinforcement exists only in tension area near the support. This means that concrete behavior in most of the beam is almost like plain concrete.

Figure 14 shows the relation between load and deformation under the applied load given from the experiment and simulation by the proposed technique and the FEM[14] which is one of the most advanced FEM programs. It can be noticed easily that the proposed technique gives good agreement with the experimental results in both deformations and failure load. The results obtained by the proposed technique are relatively better than those by the FEM. The measured failure load was about 880 kN. The calculated failure load using the proposed technique is 910 kN and that by FEM is 980 kN. Moreover, the deformations before failure using the proposed technique are better than those calculated by the FEM.

Figure 15 shows the deformed shape during loading. The right-down corner of the figure shows the location of cracks obtained by the exeperiment[14]. The followings can be noticed:
1. Simulated location of diagonal tension cracks is very similar to that obtained from the experiment.
2. Locations of high compression stress concentration at the loading points and supports before failure are also obvious (overlapping between elements).

6. CONCLUSIONS

A new simplified and accurate method for nonlinear analysis of structures is proposed. The accuracy of the method is verified by comparing with experiments and other numerical techniques. This method termed Applied Element Method, has many advantages summarized in **Table 2**.

Although the shape of elements used in the simulations is square, it does not affect the crack generation or crack propagation in the material. Diagonal cracks can be obtained even if the crack direction is not parallel to the element edges. Unlike RBSM and EDEM, it was proved that the results obtained by the proposed model do not depend on the shape and arrangement of the elements used. This means that no need to guess the crack location and propagation direction before the analysis.

Inspite of simple material models used in the analysis, the obtained load-deformation relation and crack locations agree well with the experimental results. As the method is developed recently, there are not enough results compared to other numerical models. In addition, there are several issues to be discussed, such as the effects of shear transfer, shear softening and crack width. However, based on the results introduced in this paper, it can be noted that the AEM has lot of scope in following the complete structural behavior.

Table 2 Comparison between the proposed model and the FEM

	FEM	*Proposed Method*
CPU time	Short	Short
D.O.F	16 (for two 8-node elements)	6 (for 2 elements)
Cracking Model	Smeared cracks and interface cracks (physical cracks)	Only physical cracks
	Joint elements (interface elements) at large crack locations	No need for joint elements
	Joint elements location (large cracks) should be decided before analysis	No information on location of cracks is needed before analysis
	Crack propagation can not be followed accurately in smeared crack zones	Crack propagation can be followed
Modeling time	Long	Very Short compared to the FEM
Reinforcement details	Difficult to input	Can be taken into account all reinforcement details without complication.
Accuracy	High (before collapse)	At least the same as FEM before collapse, but can be extended easily to follow collapse behavior

REFERENCES

1) Meguro, K. and Tagel-Din, H: Applied element method for structural analysis: Theory and application for linear materials, Structural Eng./Earthquake Eng., Vol. 17. No. 1, pp. 21s-35s, Japan Society of Civil Engineers, April, 2000.
2) Tagel-Din, H.: A new efficient method for nonlinear, large deformation and collapse analysis of structures, Ph.D. thesis, Civil Eng. Dept., The University of Tokyo, Sept. 1998.
3) Okamura, H. and Maekawa, K.: Nonlinear analysis and constitutive models of reinforced concrete, Gihodo Co. Ltd., Tokyo, 1991.
4) Chen, W. H. and Chang, H. S.: Analysis of two dimensional mixed-mode crack problems by finite element alternating method, Computers and Structures Vol. 33. No. 6. pp. 1451-1458, 1989.
5) Dutta, B. K. and Kakodkar, A.: Use of two singular point finite elements in the analysis of kinked cracks, paper presented at the Int. Conf. on Fracture Mechanics, U.K., Vol. 2, pp. 731-737, 1991.
6) Kawai, T.: Recent developments of the Rigid Body and Spring Model (RBSM) in structural analysis, Seiken Seminar Text Book, Institute of Industrial Science, The University of Tokyo, pp. 226-237, 1986.
7) Kikuchi, A., Kawai, T. and Suzuki, N.: The rigid bodies-spring models and their applications to three dimensional crack problems, Computers & Structures, Vol. 44, No. 1/2, pp. 469-480, 1992.
8) Ueda, M. and Kambayashi, A.: Size effect analysis using RBSM with Vornori elements, JCI (Japan Concrete Institute) International Workshop on Size Effect in Concrete Structures, pp. 199-210, 1993.
9) Meguro, K. and Hakuno, M.: Fracture analyses of structures by the modified distinct element method, Structural Eng./Earthquake Eng., Vol. 6. No. 2, pp. 283s-294s., Japan Society of Civil Engineers, 1989.
10) Meguro, K. and Hakuno, M.: Application of the extended distinct element method for collapse simulation of a double-deck bridge, Structural Eng./Earthquake Eng., Vol. 10. No. 4, pp. 175s-185s., Japan Society of Civil Engineers, 1994.
11) Kupfer, H., Hilsdorf, H.K. and Rusch, H.: Behavior of concrete under biaxial stresses, ACI journal, Vol. 66, No. 8, pp. 656-666, Aug. 1969.
12) Ono, H.: Study on seismic capacity of reinforced concrete shear wall, Part 7, Relation between load history and horizontal reinforcement, Proc. of annual conference of Architectural Institute of Japan (AIJ), pp. 1601-1602, 1976. (in Japanese)
13) Muto, K.: Strength and deformations of structures, Maruzen Co. Ltd., 1965. (in Japanese)
14) Niwa, J., Maekawa, K. and Okamura, H.: Nonlinear finite element analysis of deep beams, 10th annual lecture on "FEM Analysis of Reinforced Concrete Structures", Civil Engineering Department, The University of Tokyo, 1995.